Imaging the relationship between tumour interstitial fluid velocity and microvascular perfusion with convectionMRI

Simon Walker-Samuel[1], Jake Burrell[2], Rajiv Ramasawmy[1], Peter Johnson[3], Jack Wells[1], Bernard Siow[1], Simon P. Robinson[2], Barbara Pedley[3], and Mark F. Lythgoe[1]

[1]*Centre for Advanced Biomedical Imaging, University College London, London, United Kingdom,* [2]*CR-UK & EPSRC Cancer Imaging Centre, The Institute of Cancer Research, United Kingdom,* [3]*Cancer Institute, University College London, United Kingdom*

Introduction: Tumours exhibit higher interstitial fluid pressure (IFP) than normal tissues due to the raised permeability of tumour blood vessels [1]. This reduces the hydrostatic pressure gradients normally found between blood vessels and the interstitium, which can hinder the delivery of therapeutic agents to the tumour [2]. It also results in radial convection currents through the tumour interstitium, which can result in the rapid extraction of such molecules [1]. This effect, coupled with poor vascular perfusion, can act as a significant barrier to effective drug therapy. We have recently developed a novel imaging technique named convectionMRI, which allows direct measurement of interstitial fluid velocity (IFV) without using a contrast agent. By combining this technique with arterial spin labelling (ASL), we have been able to assess the relationship between vascular perfusion and interstitial convection in two contrasting colorectal tumour xenograft models.

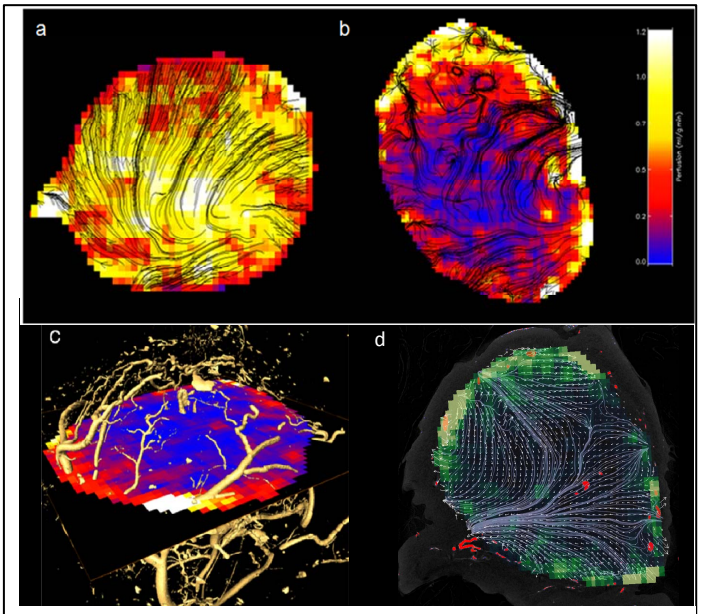

Figure 1: (a-b) Example ASL perfusion maps (colour scale) overlaid with convectionMRI streamlines (black) showing probabilistic pathways of fluid transport through the tumour interstitium in an SW1222 tumour (a) and LS174T tumour (b). **(c)** A microvascular cast scanned with micro-CT and with blood vessels volume-rendered (yellow), with a co-registered perfusion map overlaid (colour scale). Regions with high perfusion values can be seen to overlay blood vessels in the microvascular cast. **(d)** Co-registered images of blood vessels from microvascular casting (red), ASL perfusion (green), interstitial fluid velocity (IFV) vectors (white arrows) and convection streamlines (grey lines) from an LS174T tumour. The latter two parameters are derived from convectionMRI. The source of interstitial convection currents correspond to regions of high vascular perfusion.

Methods and Materials: *Animal models:* MF1 nu/nu mice were injected subcutaneously on the lower right flank with 5×10^6 SW1222 or LS174T colorectal carcinoma cells (n=6 for both). Tumours were allowed to grow for 16 days and were scanned using a 9.4T Agilent VNMRS scanner with a 39 mm birdcage coil (Rapid MR International, Columbus, Ohio). Mice were anaesthetised using isoflurane (1.25% in O_2), and core body temperature was monitored and maintained at 37° using a warm air blower. Tumours were restrained using dental paste in order to minimise bulk motion. A single coronal slice covering the largest extent of each tumour was selected from a set of multi-slice, fast spin-echo multi-slice (FSEMS) images, and was used to acquire convectionMRI and ASL data.

ConvectionMRI: In the convectionMRI sequence a global adiabatic inversion pulse is followed immediately by a slice selective inversion [4]. Following a recovery delay t_{rec} in which inverted blood flowing into the selected slice recovers to the null point (t_{rec} = ln(2)$T_{1,blood}$), a gradient echo readout is applied, during which bipolar velocity encoding gradients are applied (G = 5 G/cm, τ = 20 ms). Nulling the vascular signal with the dual inversion enables interstitial velocities to be measured using standard velocity encoding techniques [5]. The T_1 of blood was taken to be 1900 ms from previous measurements in the ventricular blood pool. Two bipolar gradient configurations were used in three orthogonal directions, the second of which were of opposite polarity to the first. The difference in phase between the two measurements, $\Delta\phi$, is proportional to IFV. The convectionMRI gradient echo readout included the following parameters: TR = 2500 ms, TE = 2.6 ms, flip angle = 30°, slice thickness = 1 mm, field of view = 35×35 mm^2, matrix size = 128×128.

ASL: Perfusion measurements were obtained using a FAIR Look-Locker ASL sequence with a single-slice spoiled gradient-echo readout [5]. Sequence parameters included: TE = 1.18 ms, TI = 110 ms, TRRF = 2.3 ms, TRI = 13 s, 50 inversion recovery readouts, localised inversion thickness = 3 mm, global inversion slice thickness = 200 mm, 4 averages. All geometric parameters were matched to the convectionMRI sequence.

Microvascular casting: Following MRI scanning, mice were systemically perfused with an intravascular, radiopaque casting material (Microfil, Flowtech Inc.). Tumours were excised and scanned using μCT at an isotropic resolution of 6 μm (Skyscan).

Post-processing: Data were analysed using in-house software written in IDL. IFV was calculated using $v = \Delta\phi / (\gamma \Delta M_1)$ (where γ is the gyromagnetic ratio and ΔM_1 is the difference in first order velocity gradient moments). Maps of IFV streamlines were calculated and visualised using the iVector tool in IDL. Perfusion maps were calculated using the quantitative model described by Belle *et al.* [4]. Soft tissue was visible at low signal intensity in μCT and was used for alignment with FSEMS data. This, in turn, allowed the alignment of IFV and perfusion maps with microvascular cast data. Blood vessels were segmented from μCT data by simple thresholding, allowing surface-rendered, 3D vessel networks to be constructed. All three-dimensional registration and visualisation was performed in Amira (Visage Imaging).

Results and Discussion: ASL measurements revealed a median perfusion of 0.28 ± 0.16 ml/mg.min in SW1222 and 0.15 ± 0.11 ml/mg.min in LS174T tumours. In LS174T tumours perfusion was higher towards the periphery, whilst in SW1222, perfusion was more homogeneously distributed (see Figs. 1a and b). This pattern of vascular organisation was also evident in vascular casts, and is consistent with previous studies in these tumour types that show SW1222 tumours to be more homogeneously vascularised and better perfused than LS174T tumours [3]. As illustrated in Fig. 1c, highly perfused regions were coincident with the location of large vessels in microvascular casts, although non-perfused vessels were also visible at the centre of tumours.

IFV streamline maps estimate the probabilistic path of fluid through the interstitium, and examples are shown overlaid on perfusion maps in Figs. 1 and b. These reveal convection pathways emanating from regions with high perfusion and flowing through 'corridors' of decreasing perfusion gradient. This was particularly evident in SW1222 tumours, which show a typical 'radial' convection pattern. Conversely, LS174T tumours showed a laminar convection from one edge to the other. A multi-functional map overlaying a microvascular cast cross-section, perfusion values and IFV streamlines from an LS174T tumour, is shown in Fig. 1d. This image clearly illustrates the correspondence between perfusion and the spatial patterning of IFV. As IFP is proportional to the spatial gradient of IFV, these results are consistent with the hypothesis that high tumour interstitial fluid pressure is driven by microvascular pressure [1].

Conclusion: **C**ombining convectionMRI (a novel imaging method for quantifying IFV) and ASL has enabled the relationship between tumour vascular perfusion and interstitial convection to be non-invasively evaluated. The observed relationship between perfusion and IFV patterns is consistent with the hypothesis that raised vascular permeability and microvascular pressure is the source of raised interstitial fluid pressure in tumours. This combination of techniques has the potential to probe unexplored aspects of tumour biology and to elucidate barriers to drug delivery.

Acknowledgements: King's College London and UCL Comprehensive Cancer Imaging Centre, CR-UK & EPSRC, in association with the MRC and DoH (England), British Heart Foundation. **References:** [1] Boucher *et al.* Cancer Res., 1990;50(15) [2] Jain, Cancer Metastasis Review, 1990;9(3) [3] Folarin *et al.*, Microvasc Res. 2010;80(1), [4] Belle, *et al.* J Magn Reson Imaging 1998;8.